

LA-UR-17-22073

Approved for public release; distribution is unlimited.

Title: SURF Model Calibration Strategy

Author(s): Menikoff, Ralph

Intended for: Report

Issued: 2017-03-10



SURF MODEL CALIBRATION STRATEGY

RALPH MENIKOFF

March 1, 2017

Abstract

SURF and SURFplus are high explosive reactive burn models for shock initiation and propagation of detonation waves. They are engineering models motivated by the ignition & growth concept of high spots and for SURFplus a second slow reaction for the energy release from carbon clustering. A key feature of the SURF model is that there is a partial decoupling between model parameters and detonation properties. This enables reduced sets of independent parameters to be calibrated sequentially for the initiation and propagation regimes. Here we focus on a methodology for fitting the initiation parameters to Pop plot data based on 1-D simulations to compute a numerical Pop plot. In addition, the strategy for fitting the remaining parameters for the propagation regime and failure diameter is discussed.

1 Introduction

A high explosive (HE) burn model for initiation and propagation of detonation waves consists of three parts: i. Equations of state (EOS) for the reactants and products. ii. A mix model for partly burned HE; i.e., pressure $P(V, e, \lambda)$ where V is the specific volume, e is the specific internal energy and λ , the reaction progress variable, is taken as the mass fraction of the products. iii. Rate equations for the reaction progress variable, $\frac{d}{dt}\lambda = \mathcal{R}$, and any internal state variables of the burn model. Rates are functions of the state variables; (V, e, λ) and model dependent state variables. The lead shock pressure for the SURF model and the carbon cluster reaction progress variable for the SURFplus model are examples of model dependent state variables. Typically, model rates are fitting forms with parameters calibrated to reproduce some set of experimental data.

The first step in calibrating a burn model for a specific HE is determining the EOS from the available data; typically, the shock locus or isothermal compression data for the reactants, and the overdriven detonation locus and detonation release isentrope data for the products. For the second step, pressure-temperature equilibrium is a mix model commonly used for HE. Here, the focus is on the third step or calibrating an empirical fitting form for a burn rate. Moreover, we consider only the SURF [Shaw and Menikoff, 2010, Menikoff and Shaw, 2010] and SURFplus [Menikoff and Shaw, 2012] models.

An important property of the SURF model is that there is a partial decoupling between model parameters and detonation wave properties. This greatly simplifies the methodology that can be used to calibrate the burn model. It also alleviates issues when correlated variations of parameters give nearly the same results; *i.e.*, when the available calibration data is not sufficient to fully determine all the model parameters.

The SURF model parameters are discussed in section 2. An important feature of the SURF rate is that there are 3 pressure regimes that dominate different detonation phenomenon. The calibration strategy, outlined in section 3, takes advantage of this. The idea is to start by estimating the transition pressures that define the regimes and then to calibrate reduced sets of independent rate parameters sequentially for the shock ignition regime followed by parameters for the detonation wave propagation regime. However, an additional parameter is needed to account for the failure diameter and shock initiation with complex drive conditions such as a curved shock front followed by a pressure gradient; see for example [Menikoff, 2016d]. This weakly couples the calibration of the parameters for the different regimes, and will require an iteration in which the transition pressures are varied and the regime parameters readjusted.

Here we focus on the two parameters that dominate shock ignition and fitting them to Pop plot data; *i.e.*, run-distance to detonation driven by a sustained shock. Features of the Pop

plot and the pressure regime that dominates the initiation regime are discussed in section 4. In addition, we review the procedure previously described for numerically computing the Pop plot corresponding to a burn model [Menikoff, 2015a], and a metric for comparing numerical results with Pop plot data.

Calibrating a model amounts to finding parameters that minimizes a metric for goodness of fit. The dependence of the metric on model parameters can be very nonlinear. Typically, minimizing the metric requires an iterative scheme. Evaluating the metric for a given parameter set is computational expensive as it requires several hydro simulations. Qualitative properties of the metric as a function in parameter space, such as its smoothness or whether it has one or more local minimum, are important for designing an efficient algorithm for model calibration.

A natural first step for determining properties of the Pop plot metric is to pick an illustrative HE and simply evaluate the metric over a grid in the 2-D initiation parameter space. PBX 9501 and PBX 9502 are used as illustrative HE for the SURF and SURFplus models, respectively. The implementation of the SURF and SURFplus models have been verified in the xRage code [Menikoff, 2016a,b,c], and it is used for the numerical simulations needed to evaluate the metric.

Numerical results, shown in section 5, are that the Pop plot metric for the SURF model is fairly smooth. The grid point with the minimum metric can be used as the calibration for the value of the two initiation parameters. If greater accuracy is needed, the grid evaluation can be used to set bounds on the parameters for an iterative algorithm such as the downhill simplex method. The brute force approach of evaluating the metric over a grid is only feasible for a 2-D parameter space. It has the advantage that points on the grid representing different parameter sets can be computed in parallel on separate processes of a high performance computer node.

The propagation regime parameters can be fit to curvature effect data; *i.e.*, detonation speed as a function of front curvature. This can be done by solving a system of ODEs for the reaction-zone profile; in the context of the SURFplus model see [Menikoff and Shaw, 2012]. The propagation regime is affected to some extent by a parameter needed for the SURF model to fit the measured failure diameter and complex shock initiation data. As previously mentioned, depending on the desired accuracy, calibration may requires an iteration in which the transition pressures are varied and the regime parameters readjusted.

The last section summarizes the approach to calibrating the SURF model. Additional issues related to calibration are also discussed. These include the effect of resolution and the choice of metric. In addition, for some explosives a complete set of calibration data may not be available. In this case, estimating the transition pressures and fitting a small number of parameters based on the Pop plot may be the best one can do with the limited data available.

2 SURF rate

The fitting form for the SURF rate has evolved from that given in the original formulation [Menikoff and Shaw, 2010] to a form that better fits the Pop plot at low pressure [Menikoff, 2016a, App. D], to the fitting form used here. The number of parameters and main features of the rate are essentially the same.

The new fitting form is motivated by the observation that for the model parameters that fit shock initiation data, the burn rate vs shock pressure in the ignition regime is very nearly linear on a log-log plot. This implies the rate is proportional to the shock pressure to a power. Other models, in particular, Ignition & Growth [Lee and Tarver, 1980, Tarver et al., 1985] and WSD [Wescott et al., 2005] take the rate to be proportional to the pressure to a power, though for these models the rate depends on the local pressure rather than the shock pressure for the SURF model.

The reaction progress variable for the SURF model is determined as a function of a dimensionless reaction-scale variable s and a reaction-scale function g(s);

$$\lambda = g(s) , \qquad (1a)$$

$$\frac{\mathsf{d}}{\mathsf{d}t}s = \tilde{f}(p_s, p) = f(p_s) \cdot \begin{cases} 0, & \text{for } p \le 0\\ \left[\frac{p}{p_s}\right]^n, & \text{for } 0 (1b)$$

where $f(p_s)$ is a shock-strength function representing the number density of hot spots activated by the lead shock, n is a model parameter and p_s is the shock pressure from the shock detector algorithm, see [Menikoff, 2016a]. The parameter n affects the failure diameter and shock initiation when there is a large pressure decreasing gradient behind the lead shock.

The fitting forms used for the reaction-scale function is taken to be

$$g(s) = 1 - exp(-s^2)$$
 (2)

This can be associated with cylindrically expanding deflagration wavelets from randomly distributed hot spots. The standard burn rate is obtained by the chain rule:

$$\mathcal{R}(p_s, p, \lambda) = \frac{\mathsf{d}}{\mathsf{d}t}\lambda = \frac{\mathsf{d}}{\mathsf{d}s}g(s) \cdot \frac{\mathsf{d}}{\mathsf{d}t}s \tag{3a}$$

$$= 2 \left[-\ln(1-\lambda) \right]^{1/2} (1-\lambda) \cdot \tilde{f}(p_s, p) . \tag{3b}$$

The λ -dependence of this rate enables the model to fit embedded velocity gauge profile data for shock-to-detonation transition (SDT) experiments [Menikoff and Shaw, 2010].

With pressure and time scales p_{scale} and t_{scale} , respectively, the new fitting form for the shock-strength function is given by

$$f(p_s) = \begin{cases} 0 & \text{for } p_s \leq p_0, \\ c_{low} \left[\frac{p_s - p_0}{p_{\text{scale}}} \right]^{f n_{low}} & \text{for } p_0 < p_s \leq p_{low}, \\ c \left[\frac{p_s}{p_{\text{scale}}} \right]^{f n} & \text{for } p_{low} < p_s \leq p_1, \\ f(p_1) \cdot \left[1 + df_1 \left(1 - \exp\left[-B_2 \cdot \frac{p_s - p_1}{p_{\text{scale}}} \right] \right) \right] & \text{for } p_1 < p_s. \end{cases}$$

$$(4)$$

With derived parameters

$$fn_{low} = \left[1 - p_0/p_{low}\right]^{fn},$$

$$c_{low} = c \cdot (p_{low}/p_{scale})^{fn} \cdot \left[\frac{p_{scale}}{p_{low} - p_0}\right]^{fn_{low}},$$

$$B_2 = \frac{B}{df_1} \cdot \frac{p_{scale}}{p_1} \cdot fn,$$

f and f' are continuous at p_{low} , p_1 , and also at p_0 if $fn_{low} > 1$. Asymptotically, the rate goes to $f(p_1) \cdot [1 + df_1]$ for large p_s .

The model has a total of 4 dimensionless parameters, n, $C = c \cdot t_{\text{scale}}$, fn, df_1 , and 3 pressure transition points $P_0 = p_0/p_{\text{scale}}$, $P_{low} = p_{low}/p_{\text{scale}}$, $P_1 = p_1/p_{\text{scale}}$ in units of p_{scale} . There are 4 pressure regimes (as seen in fig. 1):

- 1. $P_s \leq P_0$, sub-critical hot spot regime. Lead shock is too weak to generate active hot spots; *i.e.*, hot spots that trigger deflagration wavelets. The rate is zero, so no parameters.
- 2. $P_0 < P_s \le P_{low}$, low pressure cutoff regime. Rate is determined by continuity at P_0 and P_{low} , so no additional parameters.
- 3. $P_{low} < P_s \le P_1$, shock initiation regime. This pressure interval dominates the Pop plot; *i.e.*, shock initiation driven by a sustained shock. Rate is determined by 2 parameters C and fn.

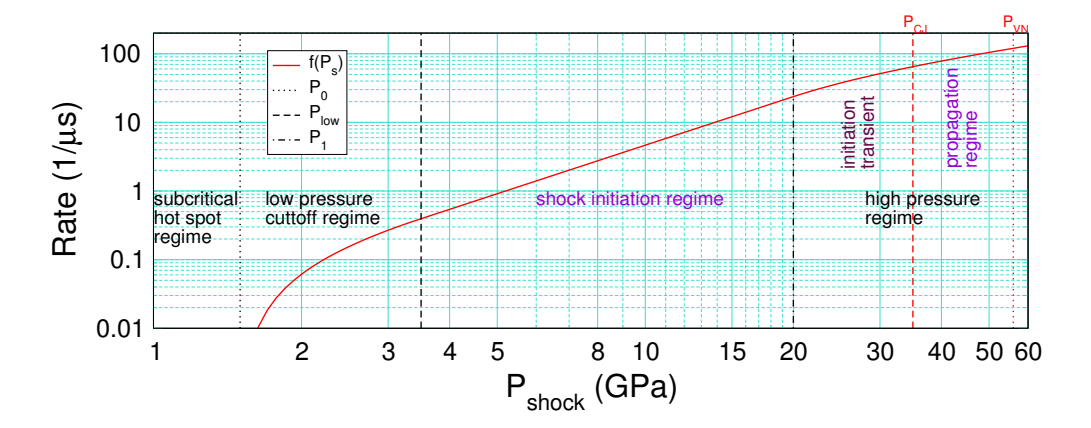


Figure 1: Illustrative example of SURF shock-strength function $f(P_s)$ for PBX 9501. Pressure transitions: $P_0 = 1.5$, $P_{low} = 3.5$ and $P_1 = 20$. For the EOS used to calibrate the rate, the CJ and VN spike pressure are 35 and 56 GPa, respectively.

4. $P_1 < P_s$, high pressure regime.

The rate is determined by 1 parameter df_1 and continuity at P_1 . The asymptotic rate corresponds to saturating or activating all potential hot spots. The pressure subinterval, $P_1 < P_s < P_{CJ}$, corresponds to a transient regime at the end of a shock-to-detonation transition. There is no rate data in this regime. The transient occurs sufficiently fast that the rate in this subinterval has a small effect on SDT with a sustained shock; *i.e.*, the Pop plot. However, it can affect other transients such as occurs when a detonation wave turns a corner.

The rate is critical when the shock pressure is between the CJ pressure and VN spike pressure. This pressure subinterval determines the reaction-zone width of a propagating underdriven detonation wave. The reaction-zone width largely determines the curvature effect; *i.e.*, the detonation speed as a function of front curvature, see [Bdzil and Stewart, 2007]. Hence, the key properties of propagating detonation waves are determined by the high pressure regime.

3 Calibration strategy

The fitting form for the SURF rate has two types of parameters:

- 1. Pressure transition points for the regions shown in fig. 1.
- 2. Rate parameters within each region.

Given estimates of the transition pressures, the small number of rate parameters within a region can be determined independently from those of the other regions.

The pressure transition parameters can be estimated as follows: The bounds on the shock initiation regime (p_{low} and p_1), should be close to the minimum and maximum pressures for shock-to-detonation transition experiments determining the Pop plot. As discussed in the next section, STD data is only sensitive to the rate in the shock initiation pressure regime.

To extend the rate to the low pressure cutoff regime, only the transition pressure p_0 is needed. If no data is available then p_0 can be taken as 0. The important point is that the choice of p_0 has no affect on fitting the standard linear Pop-plot initiation regime.

Extending the rate to the high pressure regime requires only one parameter df_1 . This can be chosen to get a sufficiently large rate at p_{vn} to match experimental data for the reaction-zone width of a propagating CJ detonation wave; see for example [Gustavsen et al., 1998]. The reaction-zone width largely determines the curvature effect.

More generally, the parameter df_1 can be adjusted to get the best match to $D_n(\kappa)$. The SURFplus parameters are needed to get the shape of the $D_n(\kappa)$ curve for small κ when carbon clustering contributes to the energy release. The parameter fit can be done by solving ODEs for the reaction-zone profile for given front curvature κ ; in the context of the SURFplus model see [Menikoff and Shaw, 2012]. Since the carbon clustering rate is slow compare to the SURF hot-spot rate, the SURFplus reaction has only a small effect on shock initiation. It does give rise to a transient after a shock-to-detonation transition in which the detonation pressure builds up to its steady state value.

There are two complications with estimating p_1 . First, the rate in the initiation transient regime of fig. 1 can affect the failure diameter and slow burning regions when a detonation wave turns a corner. As a rule of thumb, p_1 should be between $\frac{1}{2}$ and $\frac{2}{3}$ of p_{cj} . This is based on the observation that the boundary pressure for an unconfined rate stick just over the failure diameter is about $\frac{1}{2}P_{cj}$. Typically, this is above the maximum pressure on the Pop plot. If P_1 is too large than the rate will be too large in the regime that controls the failure diameter leading to a model failure diameter that is smaller than the measured failure diameter.

Second, the parameter n in Eq. (1b) is needed to fit shock initiation when there is a pressure decreasing gradient behind the initiating shock. As shown in the next section, n has a small effect on the Pop plot (sustained shock driving SDT) since there is a pressure increasing gradient behind the lead shock. However, the parameter n does affect the reaction-zone width of a propagating detonation wave since the pressure decreases in the reaction zone and p_{cj}/p_{vn} can be as low as 0.6. Hence, n will affect the curvature effect.

Consequently, one may need 'outer iterations' for which the parameters p_1 and n are varied and 'inner iterations' for refitting the sustained shock initiation and propagation regimes. It

should be noted that fitting the Pop plot initiation regime and curvature effect for the propagating regime only requires 1-D simulations. In contrast, the failure diameter and corner turning require 2-D simulations, which computationally are much more expensive. Thus, for efficiency of calibration algorithm, there is good reason to think in terms of 'inner' and 'outer' iterations.

4 Properties of Pop plot

The Pop plot characterizes a key property of shock initiation; namely, run-distance to detonation driven by a sustained planar shock. As first observed by Ramsay and Popolato [1965], on a log-log plot the data for run distance vs initial shock pressure can be fit with a straight line. Moreover, Pop plot data are available for many explosives; see for example [Gibbs and Popolato, 1980, Part II, sec. 4.1]. Here we discuss the pressure regime which is constrained by Pop plot data.

Experimental data for the Pop plot cover a limited range of pressures. At high pressure the run-distance gets small and difficult to measure. Typically, the data cuts-off when the run distance is down to 1 or 2 mm. The low pressure limit is due to the difficulty of maintaining the pressure behind the shock driving the HE. This is largely determined by the width of the HE and rarefactions from the sides. Typical run distances are less than 30 mm. The largest HE width for a sustained shock has been achieved using a 155 mm howitzer to launch a flyer plate that drives a shock in the HE [Vandersall et al., 2010]. This allows for a run distance up to 100 mm.

At low shock pressures the run-distance increases over the standard linear fit to the Pop plot; see [Vandersall et al., 2010, fig. 15]. Though shown for HMX based explosives, this is expected to be a general property for solid explosives since the void collapse mechanism for generating hot spots breaks down for pressures comparable to or less than the yield strength of an explosive grain.

The low pressure cut-off regime in the SURF rate is intended to capture the breakdown in the linearity of the Pop plot. An illustrative example of the effect of the low pressure SURF rate on the model Pop plot is shown in fig. 2. It is important to note that the cutoff does not affect the Pop plot for $p_s > p_{low}$.

We note that the experimental data used to fit the linear regime of the Pop plot displays a scatter of about 10 per cent in both run distance and time to detonation; see [Gustavsen et al., 2006] fig. 10 and Table II columns x^* , t^* for experimental measurements and x^* predicted, t^* prediction for Pop plot fit. Some of the scatter stems from the fact that solid explosives are heterogeneous material with statistical variations in the micro-structure, and each data point corresponds to a different sample. The scatter is suppressed by the log-log scale of the Pop plot.

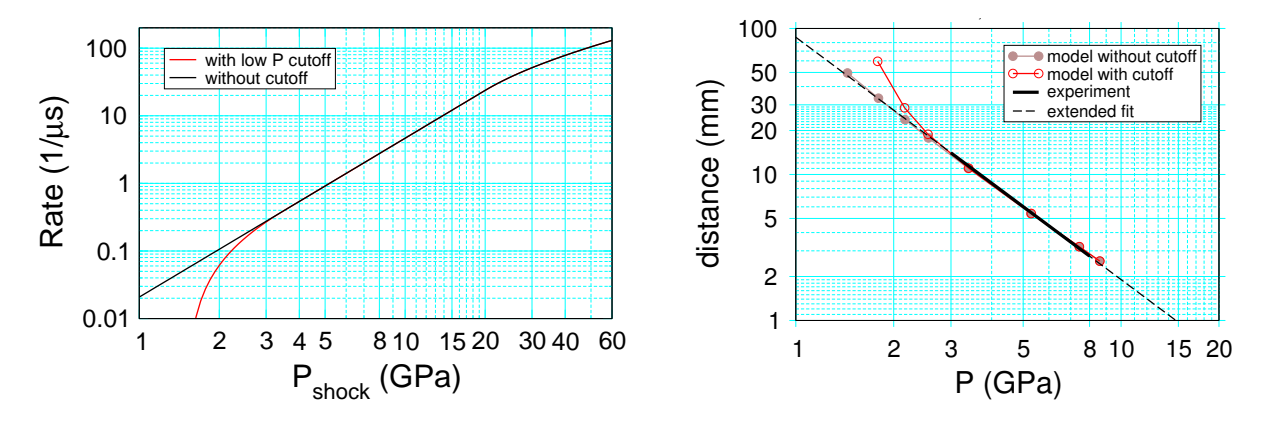


Figure 2: SURF rate Eq. (4) for PBX 9501 and numerical Pop plot showing the effect of low pressure cutoff. The cutoff parameters are $p_0 = 1.5$ GPa and $p_{low} = 3.5$ GPa. Without the cutoff, $p_0 = p_{low} = 0$.

4.1 Model Pop plot

The model Pop plot can be determined numerically by simulating shock-to-detonation transition gas-gun experiments [Menikoff, 2015a]. With different flyer plate velocities, each simulation gives one point on the Pop plot. The shock detector for the SURF model provides as a diagnostic the position, time and pressure whenever a shock is detected in a cell. This determines the lead shock trajectory, which can then be projected into various two-dimensional planes. As an illustrative example, the trajectories of $P_s(x)$ and x(t) are shown in fig. 3.

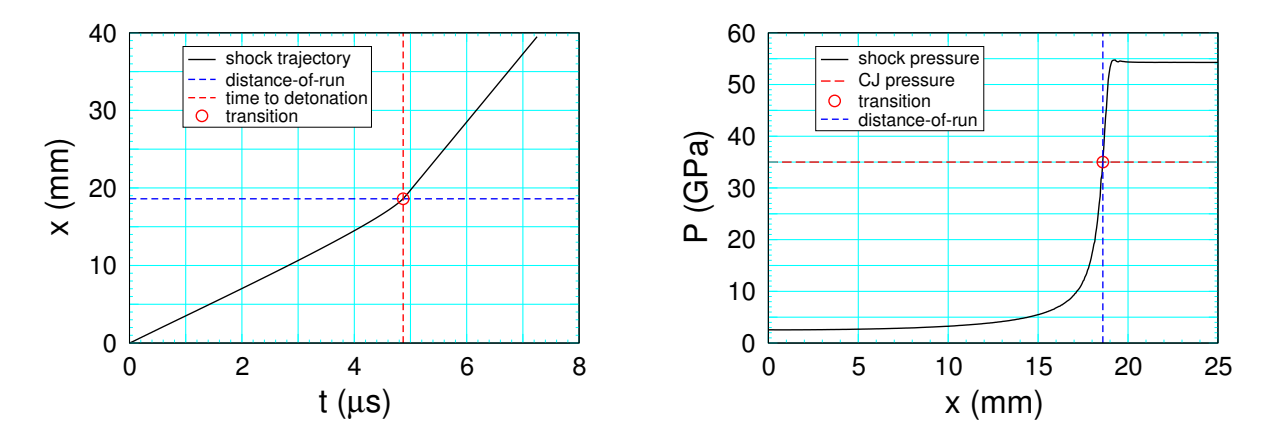


Figure 3: Illustrative trajectories of the lead shock in the x-t plane and p_s -x plane for a shock-to-detonation transition simulation with PBX 9501 using the SURF model. For model CJ pressure is 35 GPa. The circle is taken as the transition point to the detonation wave.

Experimentally, x(t) is measured and the transition to detonation is taken to correspond to the abrupt change in the slope of x(t). Typically, the trajectory is fit to a functional form to filter out noise, and then a criterion such as the point of maximum acceleration (inflexion point in the slope) is taken to correspond to the transition point for determining the distance-of-run to detonation and the time to detonation.

It is noteworthy that the lead shock pressure rises slowly at first and then abruptly transits to the von Neumann spike pressure of a detonation wave. The shape of the pressure trajectory is similar to that of the temperature vs time for a constant volume burn with an Arrhenius reaction rate. The slow pressure rise can be thought of as analogous to an induction zone and the rapid pressure rise as the onset of a runaway reaction or transition to detonation.

We will take the point on the pressure trajectory with the CJ pressure as the transition point for determining the distance-of-run to detonation. The steepness of the slope dP_s/dx implies that the run distance is not sensitive to the pressure threshold used to determine the transition point. It also implies that the burn rate in the vicinity of the CJ pressure is sufficiently large that fitting the Pop plot is not sensitive to the high pressure regime of the SURF rate.

Transition pressures

The rate parameters c and fn can be determined to fit Pop plot data for a range of values for the pressure transition points p_0 , p_{low} and p_1 of Eq. (4). Based on the phenomenology described above, a good rule of thumb is that p_{low} should be set near the minimum pressure for the linear regime of the Pop plot. The transition pressure p_0 can be set based on either available low pressure data or intuition. Lacking either of the above, p_0 can be set to zero without affecting the fit to the linear regime of the Pop plot.

A good rule of thumb for p_1 is to set it between $\frac{1}{2}$ and $\frac{2}{3}$ of P_{cj} . Typically, this is larger than the maximum pressure for Pop plot data and comparable to the boundary pressure for a detonation wave in a rate stick with diameter just above the failure diameter. Then the parameter df_1 can be set to give a sufficiently high rate at P_{vn} to get the physical reaction-zone width for a propagating detonation wave.

Pop plot metric

Since the Pop plot is on a log-log scale, the natural error to associate with a pressure point is

$$\ln(x_{sim}) - \ln(x_{exp}) = \ln(x_{sim}/x_{exp}) = \ln(1 + [x_{sim} - x_{exp}]/x_{exp})$$

 $\approx [x_{sim} - x_{exp}]/x_{exp}$.

Therefore, we take the metric for calibrating shock initiation parameters to be the root mean square of the relative error in run distance;

metric =
$$\left[N^{-1} \sum_{i=1}^{N} \left(\frac{x_{sim}(P_i) - x_{exp}(P_i)}{x_{exp}(P_i)} \right)^2 \right]^{1/2} ,$$
 (5)

where N is the number of points used to compute the numerical Pop plot and P_i is the initial shock pressure for the i^{th} SDT simulation. Run distance, x_{sim} , is determined from the shock pressure trajectory (as illustrated in fig. 3) with the CJ pressure as threshold for detonation, and x_{exp} is the run distance from the experimental Pop plot.

We note that the functional form of the burn rate does not guarantee the model Pop plot will be a straight line. In order for the metric to be sensitive to the shape of the model Pop plot, we choose N=5 for computing the metric with the points covering the range over which the experimental Pop plot is a straight line.

4.2 Embedded velocity gauges

Shock-to-detonation transition experiments with embedded velocity gauges provides information on the flow behind the lead shock [Gustavsen et al., 1999]. Numerical profiles can be calculated by simulating gas-gun experiments with Lagrangian tracer particles at the gauge locations [Menikoff, 2015b]. The shape of the profiles are determined by the model function g(s). The current fitting form Eq. (2) has been sufficient to fit profiles as shown in fig. 4.

The pressure profiles have a similar shape to the measured velocity profiles. Because there is a pressure increasing gradient behind the lead shock, the Pop plot (initiation with a sustained shock) is not sensitive to the SURF parameter n in Eq. (1b). The parameter n does affect initiation when the drive conditions are such that there is a pressure decreasing gradient behind the lead shock, such as occurs in the gap test; see for example [Gibbs and Popolato, 1980, Part II, sec. 4.2].

We note that the Ignition & Growth and WSD models assume the rate is proportional to $\lambda^{n_1}(1-\lambda)^{n_2}$. With $n_1=n_2=\frac{1}{2}$ the λ dependence is similar to that of Eq. (3b). At some future time, a more general fitting form for g(s) can be used. This would result in more than 2 parameters to fit both the Pop plot and embedded gauge profiles. Calibration would then require an iterative algorithm to determine the SURF ignition parameters.

In addition, one would need to choose a metric that weights multiple gauges from different experiments taking into account uncertainties associated with each data set. Alternatively, the metric can aim to capture features of each profile, such as shock strength and arrival time, and

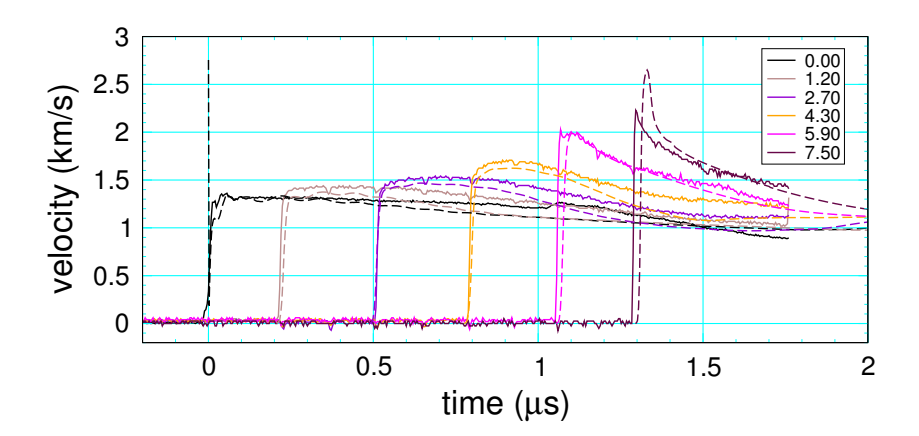


Figure 4: Illustrative example of fit to embedded gauge data; SURFplus model for PBX 9502 and Shot 2s40 [Menikoff, 2015b, fig. 8]. Solid lines are experiment and dashed lines are calibration. Gauge position are given in the legend.

peak velocity and relative time behind the shock [Handley and Christe, 2017], rather than a simple L_2 norm of the difference between experimental and numerical profiles. Also note that [Handley and Christe, 2017] use the particle swarm optimization method to find the best fit.

5 Numerical results

In contrast to other HE burn models, the SURF rate depends on the shock pressure. An algorithm for detecting the lead shock is part of the SURF model. The implementation of the shock detection algorithm has been verified for the xRage code [Menikoff, 2016a]. In addition, the implementation of the SURF and SURFplus models have been verified for a propagating detonation wave (ZND reaction-zone profile followed by a Taylor wave) [Menikoff, 2016b,c]. All the simulations reported here use the xRage code.

xRage is an Eulerian adaptive mesh code. The value of input parameters that affect the grid resolutions are as follows:

- 1. $dxset = 0.4 \, mm$: Level 1 (coarsest) grid cell size.
- 2. sizemat=0.1 mm: refine down to this cell size to resolve gradients in flow.
- 3. he_zone_size= 0.025 mm: refines reaction zone down to this cell size.
- 4. he_refine_dw=0.01: refines reacting region to next level if $\frac{\Delta x}{D_{cj}} f(P_s) > dw$. This is intended to limit refinement in dead zones or slow burning regions for which the burning has a small effect on the flow. With fine resolution, a small change in the burn fraction per time step limits truncation error from the operator split treatment of the reaction source terms.

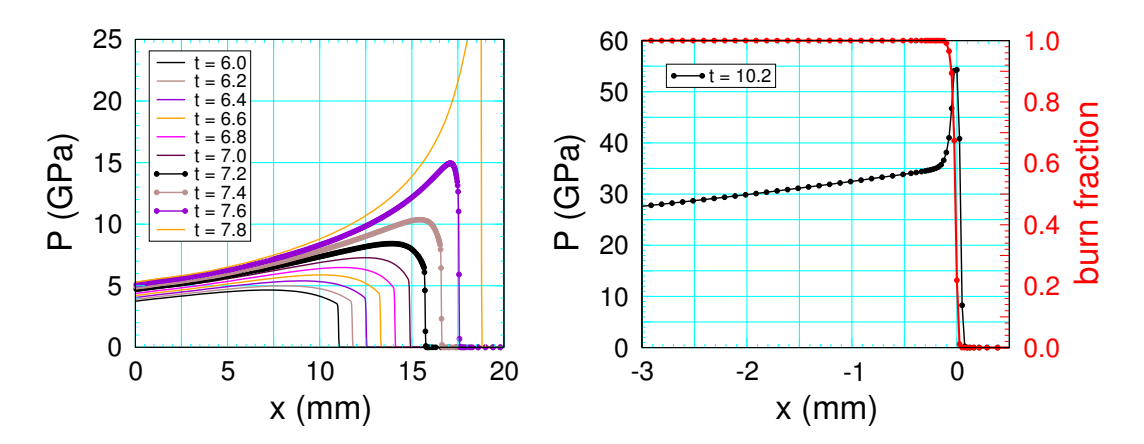


Figure 5: For PBX 9501 SDT simulation, sequence of pressure profiles at selected times and detonation wave profile. Symbols correspond to computational cells.

To illustrate the resolution used for the shock-to-detonation simulations, fig. 5 shows a sequence of pressure profiles from a SURF model simulation with PBX 9501. We note several important points:

- 1. The reaction region prior to the transition to detonation is well resolved. In contrast, there are only 4 points in the reaction zone of a detonation wave. In general, the pressure regime for shock initiation is much lower than the pressure in a detonation wave profile. Consequently, the rate is lower and a coarser resolution can be used for shock initiation than is needed to resolve the reaction zone of a propagating detonation wave.
- 2. The pressure gradient behind the lead shock gets steeper as the profile gets closer to the transition to detonation. When the magnitude of the pressure gradient is a significant fraction of the gradient in the numerical shock profile, there can be a greater inaccuracy in the detected shock pressure. This affects the reaction rate and the distance-of-run to detonation wave. For very coarse resolution (in this example, say 0.2 mm cell size) this can affect the calibration of the model parameters. In general, we have found that with the same SURF parameters, an HE is less sensitive with coarser zoning; *i.e.*, larger distance-of-run for the same initial shock pressure. 3. The accuracy of the shock detector depends to some extent on the numerical dissipation and hence can depend on the code. Thus, with coarse resolution the choice of code can affect the calibration of model parameters.

5.1 Sample parameter space for Pop plot

We use a script to automate running the simulations to generate the numerical Pop plot over grid points for the two rate parameters of the initiation regime, while the transition pressures and other SURF model parameters are held fixed. The purpose of the script is to orchestrate running simulations for each parameter set on a separate thread (two threads per processor) of a computational node with multiple processors. That is to say, to speed up the evaluation of the Pop plot metric on the parameter space grid, the simulations are run in parallel.

The script also calculates the metric and diagnostic plots for each simulation. In addition, the script has the flexibility to easily change the material EOS, the input parameters for each simulation (such as resolution and size of the computational domain) and the metric for calibrating parameters. In other words, it is straight forward to change the HE, and to study the sensitivity of the calibration to both 'fixed' HE model parameters and computational parameters.

Rather than the initiation regime parameters C and fn of Eq. (4), we use the transformed parameters (C_r, fn) where $C_r = P_r^{fn}C$. In effect, C_r corresponds to the rate $f(P_r)$. We choose P_r to correspond to the pressure at the lower end of the experimental Pop plot. Qualitatively, increasing Cr increases the rate and shifts the Pop plot down; *i.e.*, lower distance-of-run to detonation for a given initial shock pressure. Increasing fn increases the magnitude of the slope of Pop plot since the rate increase is larger at higher pressures. Because of these trends, there is only a small subregion in (C_r, fn) parameter space for which the Pop plot metric has a chance of being small and hence containing the global minimum of the metric.

Results illustrating the Pop plot metric for the SURF and SURFplus models are described next. To sample the initiation parameter space a 21x21 grid is used. This corresponds to running a total of 5x21x21 = 2205 one-dimensional simulations. At the resolution used (0.025 mm in the reaction zone), on 1 node of 16 processors (Intel Xeon E5-2670 @ 2.6 GHz), sampling the parameter space takes about 6 hours, which corresponds to 13 minutes per parameter set. The run time is dominated by the simulations with the longest distance-of-run to detonation; *i.e.*, lowest initial shock pressure.

5.2 SURF model for PBX 9501

For PBX 9501 we use the EOS specified in Appendix D of [Menikoff, 2012]. As shown by the red curves for the detonation and shock loci of fig. 8 in [Menikoff, 2008], both the reactants and products EOS are a good fit to the available data.

The common (non-initiation regime) SURF parameters for the Pop plot simulations are listed in table 1. The sampled initiation parameter space grid (with $P_r = 3$ GPa) is $0.1 \le C_r \le 0.6$ with $\Delta C_r = 0.025$ and $2 \le fn \le 3$ with $\Delta fn = 0.05$.

The Pop plot metric over this space is shown in fig. 6. We note that the metric is fairly smooth, though there is more than one local minimum, which is likely due to numerical inaccuracies in calculating the transition point to detonation. The minimum metric on the grid occurs

Table 1: Common SURF parameters for fitting PBX 9501 Pop plot simulations; see Eq. (1b) and Eq. (4).

1 GPa
$1\mu\mathrm{s}$
1.5
3.5
20.0
50.0
2.0

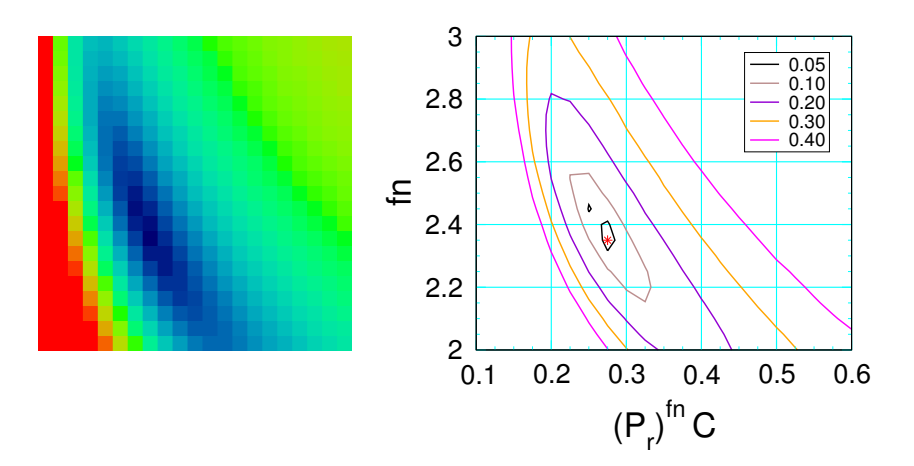


Figure 6: Color plot and contour plot of Pop plot metric for PBX 9501 as function of SURF model parameters (C_r, fn) . For color plot, blue is low and red is high. Red corresponds to parameter sets for which a shock-to-detonation transition did not occur within length of computational grid for simulation of at least one point on the Pop plot. Minimum metric on parameter space grid occurs at point marked with red star.

at $C_r = 0.275 / \mu s$ and $f_n = 2.35$. This corresponds to C = 0.0208. The rate function is shown in fig. 1.

The optimum model Pop plots, for both distance-of-run and time to detonation, are shown in fig. 7. Both are within 3 per cent of the experimental Pop plot. This is comparable to the uncertainty in the linear fit to the data.

Finally, we note from the shock trajectory shown in fig. 3 that the transition to detonation results in only a slight overshoot in the shock pressure. Moreover, after a short distance the shock pressure settles down to the steady state value, which is slightly less than the model VN spike pressure due to the under-resolved reaction zone.

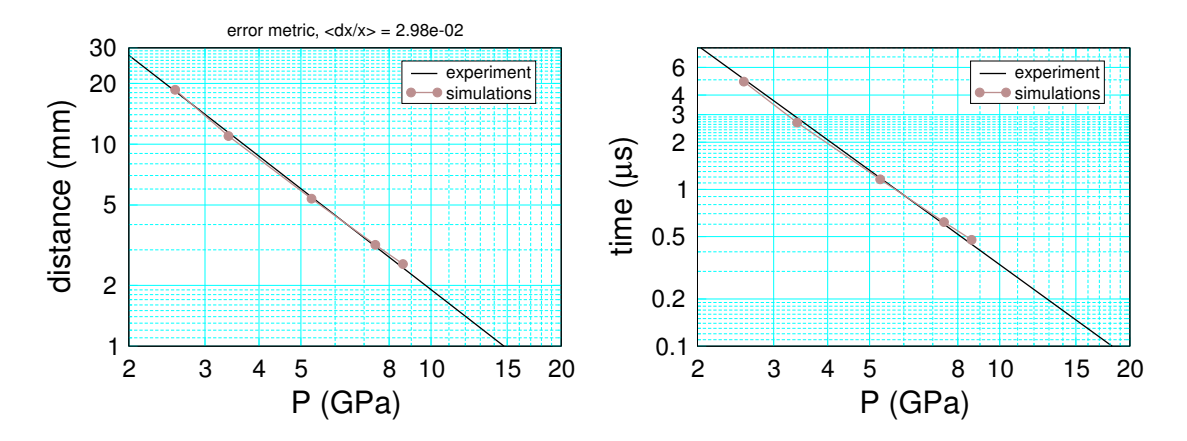


Figure 7: PBX 9501 Pop plot for SURF parameters that minimize metric.

5.3 SURFplus model for PBX 9502

For PBX 9502 we use the EOS specified in [Menikoff, 2009]. Figures 5 and 6 of the reference shows that both the reactants and products EOS are a good fit to the available data. The SURFplus model and the extra parameter values for PBX 9502 are given in appendices B.1 and D.1 of [Menikoff, 2016a]. We note that initiation is dominated by the fast SURF reaction and the second slow SURFplus reaction has little affect on the Pop plot. After the transition to detonation the SURFplus reaction gives rise to a slow transient in which the detonation state adjust to the extra energy release from the slow reaction.

The common (non-initiation regime) SURF parameters for the Pop plot simulations are listed in table 2. The sampled initiation parameter space grid (with $P_r = 8$ GPa) is $0.1 \le C_r \le 0.3$ with $\Delta C_r = 0.01$ and $3.7 \le fn \le 4.7$ with $\Delta fn = 0.05$.

Table 2: Common SURF parameters for fitting PBX 9502 Pop plot; see Eq. (1b) and Eq. (4).

p_{scale}	1 GPa
t_{scale}	$1 \mu \mathrm{s}$
P_0	6.0
P_{low}	8.0
P_1	17.5
df_1	50.0
$\mid n \mid$	3.0

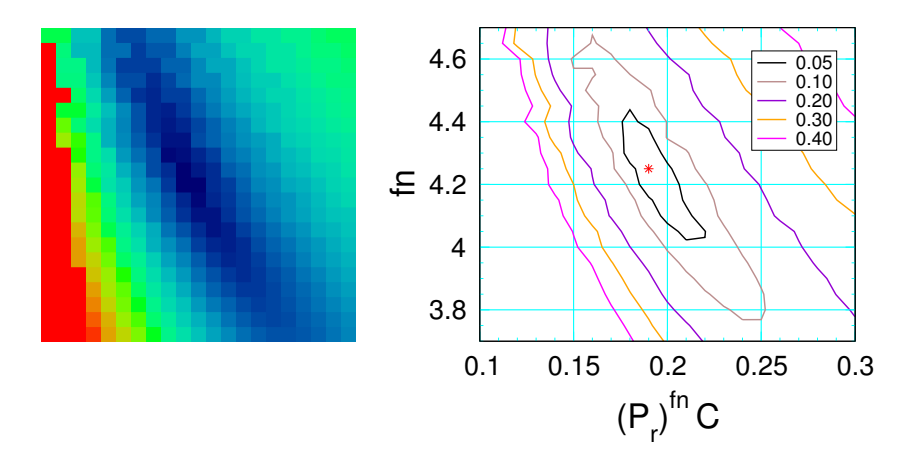


Figure 8: Color plot and contour plot of Pop plot metric for PBX 9502 as function of SURF model parameters (C_r, fn) . For color plot, blue is low and red is high. Red corresponds to parameter sets for which a shock-to-detonation transition did not occur within length of computational grid for simulation of at least one point on the Pop plot. Minimum metric on parameter space grid occurs at point marked with red star.

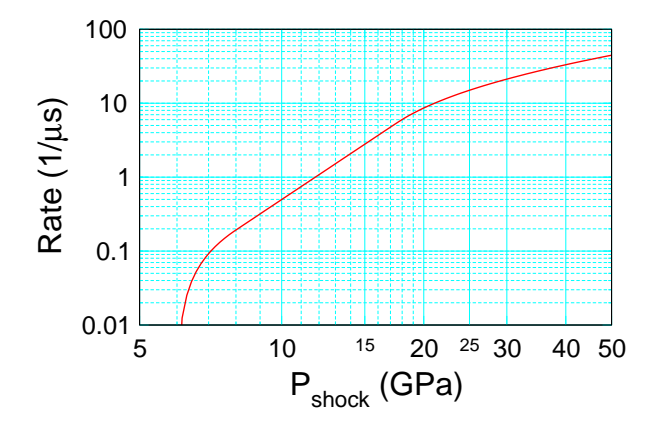


Figure 9: SURF rate for PBX 9502 with parameters that minimize Pop plot metric.

The Pop plot metric over this space is shown in fig. 8. We note that the metric is fairly smooth. Since the C_r grid spacing is $2\frac{1}{2}$ times finer than used for PBX 9501, the contours are not as smooth as those in fig. 6. This is likely due to numerical inaccuracies in calculating the transition point to detonation. The minimum metric on grid occurs at $C_r = 0.19 / \mu s$ and fn = 4.25. This corresponds to $C = 2.8 \times 10^{-5}$. The rate function is shown in fig. 9.

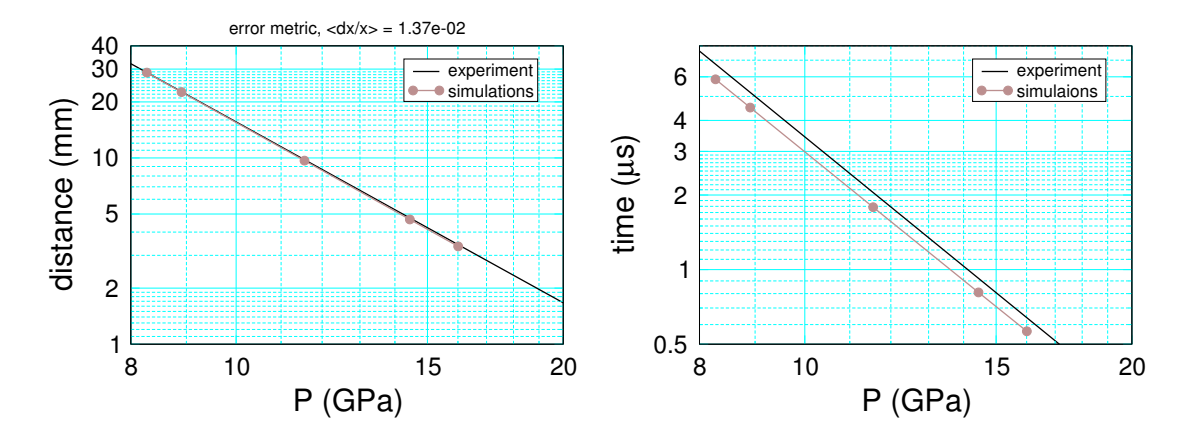


Figure 10: PBX 9502 Pop plot for SURF parameters that minimize metric.

The optimum model Pop plots, for both distance-of-run and time to detonation, are shown in fig. 10. In contrast to PBX 9501, the run-distance is fit within 1.5 percent, but the time to detonation is systematically low by about 15 per cent. This raises two question. First, should the metric for calibrating the model parameters be a weighted average of the run-distance and the run-time. Second, what is the cause of the discrepancy.

From the shock trajectory shown in fig. 11, the transition to detonation is not as abrupt as for PBX 9501, as seen in fig. 3. This is due to the rate being lower. Nevertheless, one can exclude the threshold pressure as the cause of the discrepancy since both the run-distance and run-time increase with threshold pressure and their relative change is small.

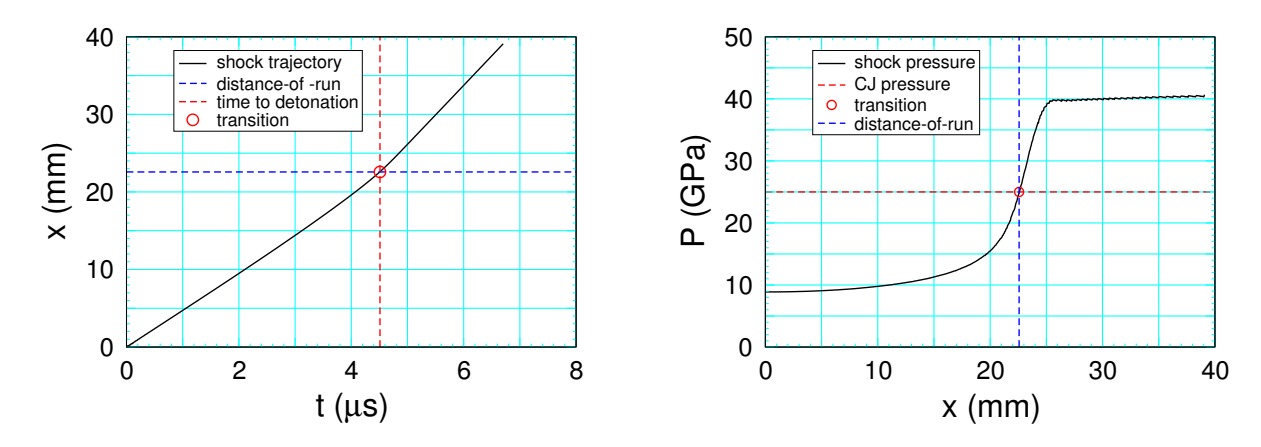


Figure 11: Shock trajectories for PBX 9502 the x-t plane and p_s -x plane. For the burn model EOS, the CJ pressure is 28 GPa. The circle is taken as transition point to the detonation wave.

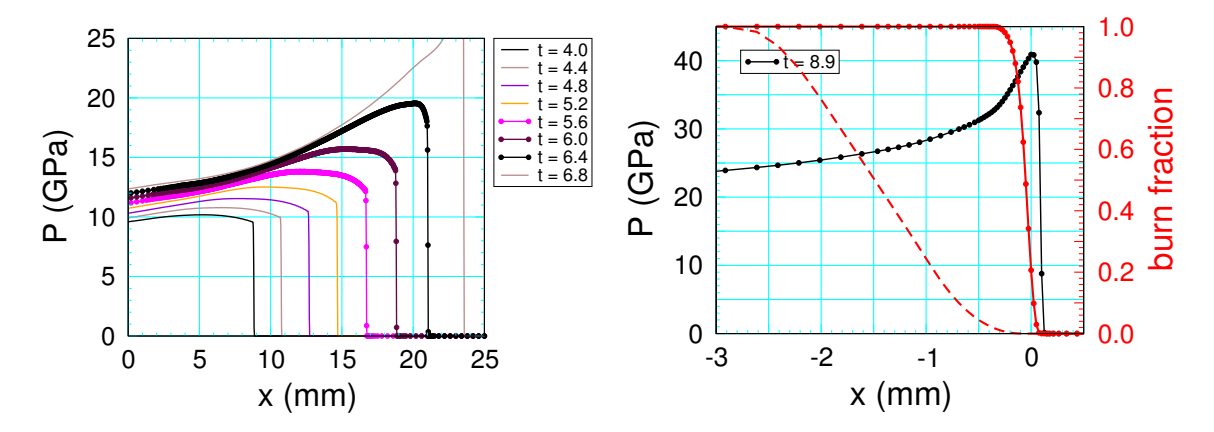


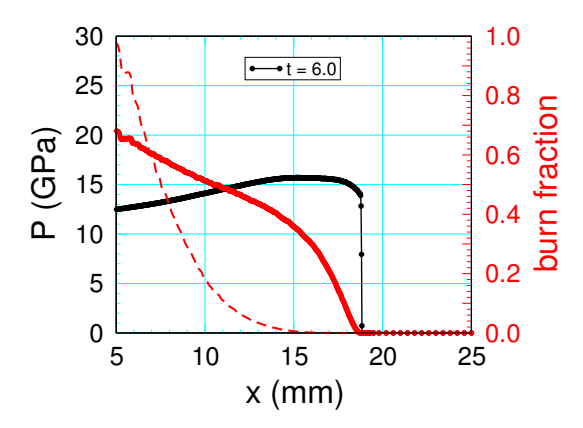
Figure 12: Sequence of pressure profiles at selected times and detonation profile. Symbols correspond to computational cells. Solid and dashed red curves are the SURF and SURFplus reaction progress variables, respectively.

Another possible cause of the discrepancy is the model reactant Hugoniot locus. Reactant Hugoniot points, even at moderate pressures, are difficult to determine accurately because reaction can bias experimental measurements of the lead shock. Rerunning simulations with $u_s(u_p)$ decreased by 5%, to the lower bound of the scatter in the data points, see [Menikoff, 2009, fig. 6], helps but is not sufficient to explain the discrepancy.

Figure 12 shows a sequence of pressure profiles from a SURFplus model simulation with PBX 9502. We note that the reaction region prior to the transition to detonation is well resolved, and in contrast to PBX 9501 the reaction zone of the propagating detonation wave is reasonably resolved. This is due to the slower rate which gives a larger reaction-zone width.

Finally, we note points related shock initiation with the SURFplus model. Profiles of the pressure and reaction progress variables before the transition to detonation are shown in fig. 13. The acceleration of the shock is due to the pressure gradient behind the front and the reaction source term in the forward characteristic equation. It can be seen that the reaction progress variables are well resolved and that the SURFplus slow reaction variable is small in the region behind the shock front that causes the shock to accelerate. Consequently, initiation is dominated by the fast SURF reaction.

The slow SURFplus variable affects the flow after the transition. As seen in the shock trajectory plot, fig. 11, the lead shock pressure slowly increases after the transition. The increase is a slow transient due to the detonation state adjusting to the added energy release from the slow reaction. The approach to steady state is slow because the flow towards the end of the detonation wave reaction zone is close to sonic.



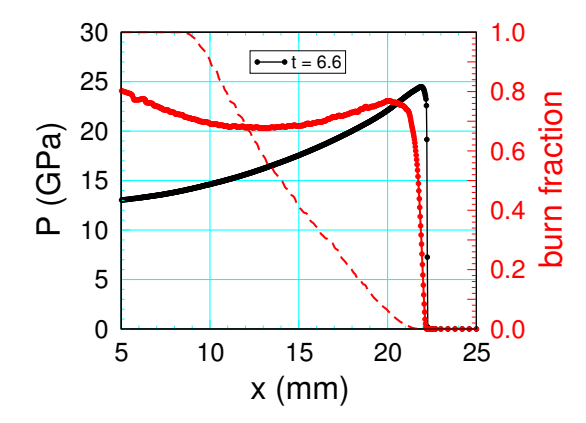


Figure 13: Profiles of pressure and reaction progress variables at two times before transition to detonation. Symbols correspond to computational cells. Solid and dashed red curves are the SURF and SURFplus reaction progress variables, respectively.

6 Summary and comments

The SURF burn rate is defined piecewise as a function of shock pressure, Eq. (4). Each pressure interval dominates a different detonation phenomenon. The two most important intervals correspond to the shock initiation regime and the propagating detonation wave regime. In each regime there are a small number of rate parameters. This results in a partial decoupling of model parameters in the sense that disjoint subsets of parameters can be used to fit different types of data.

A fairly good calibration can be obtained by estimating the transition pressures between regimes and then sequentially fitting 2 rate parameters to Pop plot data (distance-of-run to detonation for a sustained initial shock) followed by fitting 1 parameter to the reaction-zone width of a steady detonation wave or the curvature effect (detonation speed as a function of local front curvature). Fitting the Pop plot only requires 1-dimensional simulations. Fitting the curvature effect can be reduced to solving ODEs for the quasi-steady reaction-zone profile with a given curvature.

The rate parameters are partially coupled by the transition pressures and an additional parameter, n in Eq. (1b), needed to fit the failure diameter, corner turning experiments and shock initiation with complex drive conditions (curved shock front followed by a pressure decreasing gradient). Calculating these phenomena require 2-dimensional simulations. The relative computation expense motivates an approach with an outer loop in which the transition pressures and parameter n are varied, and an inner loop in which the rate parameters for the initiation and propagation regime are readjusted.

In this paper we have focused only on the first part in which the initiation rate parameters were fit to Pop plot data. Since there are only two initiation parameters and the Pop plot metric is fairly well behaved (subject to numerical noise in the simulations for determining the distance of run), the optimum initiation parameters can be determined by calculating the model Pop plot for parameters on a two-dimensional grid and then picking the grid point that minimize the Pop plot metric. This approach, while crude, is very robust and lends itself to running simulation in parallel on a multiprocessor computational node.

Several other issues need to be considered for calibrating a model to a specific explosive:

1. Mesh resolution

Typically, simulations for engineering applications do not resolve the reaction zone of a propagating detonation wave. This can affect the numerical reaction-zone width and hence the curvature effect. In 2- or 3-dimensions, for a curved detonation front, the numerical detonation speed can be a few per cent low when the detonation wave profile is captured rather than resolved; see for example [Menikoff, 2014].

Shock initiation is dominated by a lower pressure regime than occurs for propagation, and hence requires less resolution than needed for a propagating detonation wave. However, coarse resolution can introduce inaccuracies in the detected shock pressure and hence the SURF burn rate. This can influence the transition to detonation and lead to a dependence of calibrated parameter values on resolution. Similarly, the shock detector depends to some extent on the form of numerical dissipation, and parameters can also vary with the code used for the calibration simulations. We expect the magnitude of the parameter variations to decrease with finer grid resolution.

2. Uncertainty in calibration

The calibration of model parameters depends to some extent on the choice of experimental data used and on the metric for comparing experimental and simulated data. Here the focus has been on fitting Pop plot data since distance-of-run to detonation is a critical property for shock initiation. Even in this simple case, there is issue of whether the metric should be a weighted average of distance-of-run and time to detonation. For more detailed data, such as profiles from embedded velocity gauges or PDV probes, there are issues with how to weight different data sets and how to account for measurement uncertainty. Very likely finding the exact minimum of a particular metric is not worth the expense. The scheme we used of evaluating the 2 SURF initiation parameters on grid may be within the accuracy of the data.

3. Available data to calibrate model parameters

For some explosives, data on some detonation phenomena may not be available. Estimates of the pressure transitions and calibrating to Pop plot data may be best one can do when the available data is limited.

References

- J. B. Bdzil and D. S. Stewart. The dynamics of detonation in explosive systems. *Annual Rev. Fluid Mech.*, 39:263–292, 2007. 6
- T. R. Gibbs and A. Popolato, editors. *LASL Explosive Property Data*. Univ. of Calif. Press, 1980. URL http://lib-www.lanl.gov/ladcdmp/epro.pdf. 8, 11
- R. L. Gustavsen, S. A. Sheffield, and R. R. Alcon. Detonation wave profiles in HMX based explosives. In *Shock Compression of Condensed Matter 1997*, pages 739–742, 1998. 7
- R. L. Gustavsen, S. A. Sheffield, R. R. Alcon, and L. G. Hill. Shock initiation of new and aged PBX 9501 measured with embedded electromagnetic particle velocity gauges. Technical Report LA-13634-MS, Los Alamos National Lab., 1999. http://dx.doi.org/10.2172/10722. 11
- R. L. Gustavsen, S. A. Sheffield, and R. R. Alcon. Measurements of shock initiation in the tri-amino-tri-nitro-benzene based explosive PBX 9502: Wave forms from embedded gauges and comparison of four different material lots. J. Appl. Phys. 99, art. 114907, 2006. doi: 10.1063/1.2195191. 8
- C. A. Handley and M. A. Christe. Calibrating reaction rates for the CREST model. In *Shock Compression of Condensed Matter* 2015, 2017. URL http://dx.doi.org/10.1063/1.4971485. 12
- E. L. Lee and C. M. Tarver. Phenomenological model of shock initiation in heterogeneous explosives. *Phys. Fluids*, 23:2362–272, 1980. 4
- R. Menikoff. Comparison of constitutive models for plastic-bonded explosives. *Combustion Theory and Modelling*, 12:73–91, 2008. URL http://dx.doi.org/10.1080/13647830701414254. 14
- R. Menikoff. Complete EOS for PBX 9502. Technical Report LA-UR-09-06529, Los Alamos National Lab., 2009. URL http://www.osti.gov/scitech/servlets/purl/1043481/. 16, 19
- R. Menikoff. Deflagration wave profiles. Technical Report LA-UR-12-20353, Los Alamos National Lab., 2012. http://dx.doi.org/10.2172/1038128. 14
- R. Menikoff. Effect of resolution on propagating detonation wave. Technical Report LA-UR-14-25140, Los Alamos National Laboratory, 2014. URL http://dx.doi.org/10.2172/1136940.

- R. Menikoff. Numerical computation of Pop plot. Technical Report LA-UR-15-22110, Los Alamos National Lab., 2015a. URL http://www.osti.gov/scitech/servlets/purl/1209280/. 3, 9
- R. Menikoff. Shock-to-detonation transition simulations. Technical Report LA-UR-15-25266, Los Alamos National Lab., 2015b. URL http://www.osti.gov/scitech/servlets/purl/1193613/. 11, 12
- R. Menikoff. Shock detector for SURF model. Technical Report LA-UR-16-20116, Los Alamos National Lab., 2016a. URL http://www.osti.gov/scitech/servlets/purl/1234496. 3, 4, 12, 16
- R. Menikoff. Verification test of the SURF and SURFplus models in xRage. Technical Report LA-UR-16-23636, Los Alamos National Lab., 2016b. URL https://www.osti.gov/scitech/servlets/purl/1254247. 3, 12
- R. Menikoff. Verification test of the SURF and SURFplus models in xRage: Part II. Technical Report LA-UR-16-24352, Los Alamos National Lab., 2016c. URL https://www.osti.gov/scitech/servlets/purl/1258358. 3, 12
- R. Menikoff. Barrier experiments: Shock initiation under complex loading. Technical Report LA-UR-16-20140, Los Alamos National Lab., 2016d. URL https://www.osti.gov/scitech/servlets/purl/1234498. 2
- R. Menikoff and M. S. Shaw. Reactive burn models and Ignition & Growth concept. *EPJ Web of Conferences*, 10, 2010. doi: 10.1051/epjconf/20101000003. URL http://www.epj-conferences.org/articles/epjconf/pdf/2010/09/epjconf_nmh2010_00003.pdf. 2, 4, 5
- R. Menikoff and M. S. Shaw. The SURF model and the curvature effect for PBX 9502. Combustion Theory And Modelling, pages 1140–1169, 2012. URL http://dx.doi.org/10.1080/13647830.2012.713994. 2, 3, 7
- J. B. Ramsay and A. Popolato. Analysis of shock wave and initiation data for solid explosives. In Fourth Symposium (International) on Detonation, pages 233–238, 1965. 8
- M. S. Shaw and R. Menikoff. Reactive burn model for shock initiation in a PBX: Scaling and separability based on the hot spot concept. In *Fourteenth Symposium (International) on Detonation*, 2010. 2

- C. M. Tarver, J. O. Hallquist, and L. M. Erickson. Modeling short pulse duration shock initiation of solid explosives. In *Eighth Symposium (International) on Detonation*, pages 951–961, 1985.
- K. S. Vandersall, C. M. Tarver, F. Garcia, and S. K. Chidester. On the low pressure shock initiation of octahydro-1,3,5,7-tetranito-1,3,5,7-tetrazocine based plastic bonded explosives. J. Appl. Phys., 107:094906, 2010. URL http://dx.doi.org/10.1063/1.3407570. 8
- B. L. Wescott, D. S. Stewart, and W. C. Davis. Equation of state and reaction rate for condensed-phase explosives. *Journal of Applied Physics*, 98:053514, 2005. 4